Hindawi Publishing Corporation
Advances in Acoustics and Vibration
Volume 2008, Article ID 261758, 8 pages
doi:10.1155/2008/261758

Research Article

Structural Condition Monitoring by Cumulative Harmonic Analysis of Random Vibration

Yoshinori Takahashi,[1] Toru Taniguchi,[2] and Mikio Tohyama[3]

[1] *Faculty of informatics, Kogakuin University, 1-24-2 Nishi-shinjyuku Shinjyuku-ku, Tokyo 163-8677, Japan*
[2] *Information Technology Research Organization, Waseda University, 3-4-1 Okubo, Shinjuku-ku, Tokyo 169-8555, Japan*
[3] *Waseda University, Global Information and Telecommunication Institute, 1011 Okuboyama, Nishi-Tomida Honjo-shi, Saitama 367-0035, Japan*

Correspondence should be addressed to Yoshinori Takahashi, yoshinori@ieee.org

Received 11 October 2007; Revised 21 January 2008; Accepted 3 June 2008

Recommended by Lars Hakansson

Analysis of signals based on spectral accumulation has great potential for enabling the condition of structures excited by natural forces to be monitored using random vibration records. This article describes cumulative harmonic analysis (CHA) that was achieved by introducing a spectral accumulation function into Berman and Fincham's conventional cumulative analysis, thus enabling potential new areas in cumulative analysis to be explored. CHA effectively enables system damping and modal overlap conditions to be visualized without the need for transient-vibration records. The damping and modal overlap conditions lead to a spectral distribution around dominant spectral peaks due to structural resonance. This distribution can be revealed and emphasized by CHA records of magnitude observed even within short intervals in stationary random vibration samples.

1. INTRODUCTION

This paper describes spectral changes visualized in a structural-vibration system using cumulative harmonic analysis (CHA) [1] under random vibration conditions. Spectral changes in vibrations should be informative for monitoring and diagnosing system health in structures. However, it is difficult to track variations in the structural-transfer functions independent of the source-signal characteristics. This is because the transfer-function analysis of structural-vibration systems generally requires the specifications of the excitation source [2, 3].

Hirata [4] proposed a method of monitoring invisible changes in structures based on the frequency distributions of the dominant spectral components in every short interval period (SIP) under random and nonstationary vibration conditions without any specific source-signal assumptions or requirements. Changes in the modal resonance bandwidth, which represent the damping conditions for modal vibration and must therefore be a significant indicator of the health of a structure, can be evaluated from the frequency histogram of the dominant components. As variance in the distribution increases, the modal bandwidth widens, thus increasing damping. Hirata [5] also developed a method of spectral analysis, called nonharmonic Fourier analysis, for extracting the dominant low-frequency components of a vibration record in an SIP. However, spectral analysis in SIPs is normally difficult for frequency resolution and artifacts, because of time-windowing functions [6].

Resonance can be interpreted as a spectral-accumulation process of in-phase sinusoidal components with a fixed-phase lag. Therefore, as the impulse response for a resonant system is written as an infinite series from the signal-processing viewpoint, the effective length of the sequence increases as system damping decreases but this is short under heavy damping conditions. We examined the spectral-accumulation process on a sample-by-sample basis to visualize the spectral changes in the dominant modal-resonant components under random vibration.

Berman and Fincham [7] previously formulated cumulative spectral analysis (CSA) using a stepwise time-window function to evaluate the transient characteristics of

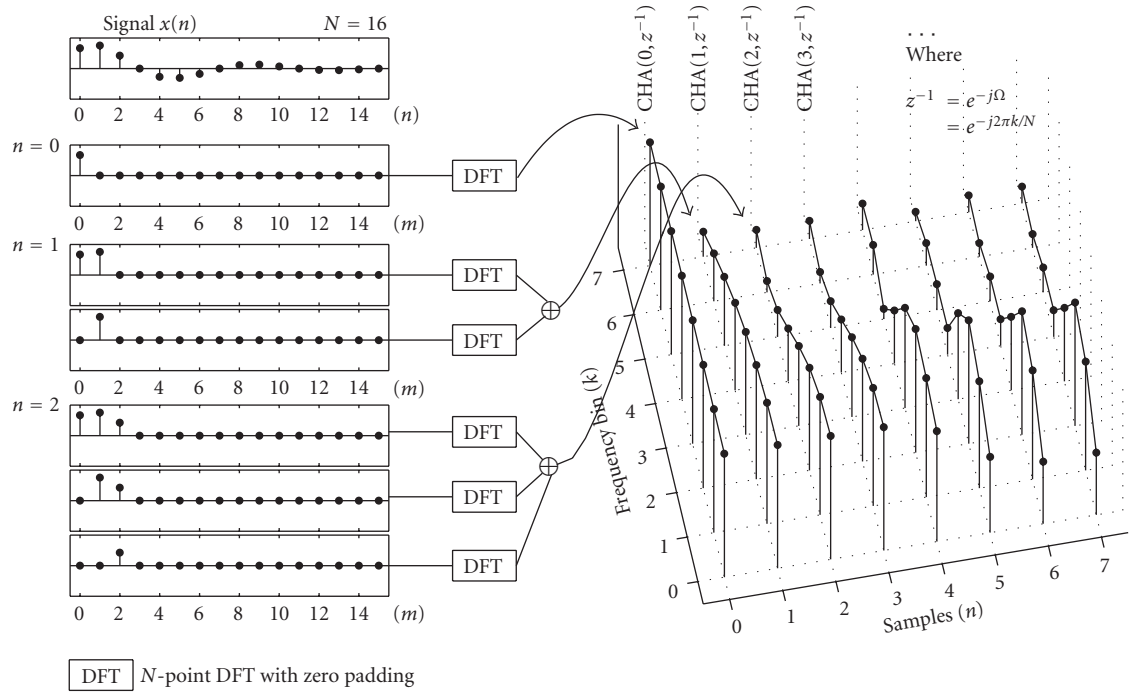

Figure 1: Schematic for cumulative harmonic analysis (CHA).

loudspeaker systems. We looked at the cumulative properties of a spectral display of vibration records including transfer function changes. In Section 2, we introduce a forgetting function into CSA instead of using a stepwise time window. We called this cumulative harmonic analysis (CHA), and its purpose was to emphasize the spectral-accumulation process, including the increasing resonant spectral peak, on a sample-by-sample basis [8]. We describe CHA's effectiveness in enabling changes in the transfer functions to be visualized through numerical simulation experiments on a single vibrating system in Section 3. In Section 4, we also describe CHA's effectiveness in a two-degrees-of-freedom (2-DOF) vibrating system. Section 5 discusses CHA visualization under conditions with damping changes.

2. FORMULATION OF CUMULATIVE HARMONIC ANALYSIS (CHA) FROM CSA

We formulate CHA by introducing a forgetting function into CSA that corresponds to the spectral-accumulation function. Assume that we have a signal sequence, $x(n)$, and define a spectral-accumulation function, $w(n)$. We define the cumulative harmonic analysis (CHA) of $x(n)$ as

$$\mathrm{CHA}(n, e^{-j\Omega}) \equiv \sum_{m=0}^{n} X(m, e^{-j\Omega}), \tag{1}$$

where

$$X(m, e^{-j\Omega}) \equiv w(m)x(m)e^{-j\Omega m}, \quad 0 \le m \le n. \tag{2}$$

Substituting a forgetting function such as

$$w(m) \equiv m + 1, \quad 0 \le m \le n, \tag{3}$$

into spectral accumulation function $w(n)$, we have

$$\begin{aligned} \mathrm{CHA}(n, z^{-1}) &= \sum_{m=0}^{n} (m+1)x(m)z^{-m} \\ &= 1x(0)z^{-0} + 2x(1)z^{-1} \\ &\quad + 3x(2)z^{-2} + \cdots + nx(n)z^{-n} \end{aligned} \tag{4}$$

in the z-plane including the unit circle where the Fourier transform can be defined. Figure 1 has a schematic of CHA. We use a triangular window as the spectral accumulation function, $w(m) = m + 1$, in this paper where the mathematical expression in the accumulation effect is simple. However, we can freely define accumulation function $w(n)$ as an exponential function, $w(m) = e^{\alpha m}$, based on the degree of necessary spectral accumulation (or forgetting effect).

The effect of the transfer-function pole on frequency characteristics can be emphasized by CHA. Assume that we have a simple decaying sequence

$$x(n) \equiv a^n \quad (n = 0, 1, 2, \ldots), \quad 0 < |a| < 1. \tag{5}$$

If we take the limit for CHA of the sequence above as

$$\lim_{n\to\infty} \mathrm{CHA}(n, z^{-1}) \equiv \lim_{n\to\infty} \sum_{m=0}^{n} (m+1)a^m z^{-m} = \frac{1}{(1 - az^{-1})^2}, \tag{6}$$

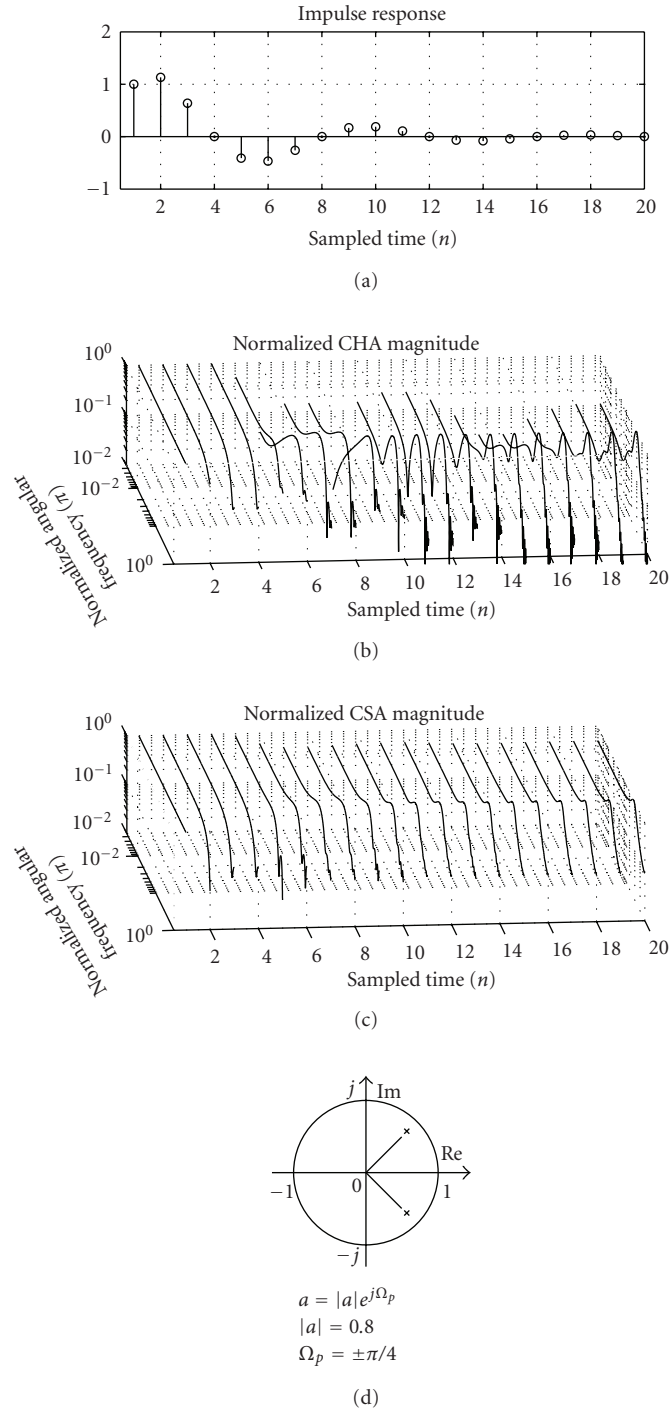

Figure 2: Samples of CHA (panel b) and CSA (panel c) magnitude displays for impulse response of single-degree-of-freedom resonance system where poles of transfer function are located at $\pi/4$ in z-plane. Panel (a) illustrates sequence of impulse responses. Maximum magnitude is normalized to unity at every instant in both panels (b) and (c) and we set $N = 800$.

then we can see that CHA virtually increases the order of the pole compared with regular discrete Fourier transform (DFT) ($w(n) = 1$)

$$\lim_{n\to\infty} \mathrm{DFT}(n, z^{-1}) = \lim_{n\to\infty} \sum_{m=0}^{n} a^m z^{-m} = \frac{1}{1 - az^{-1}}. \tag{7}$$

Consequently, the modal resonance is visualized as a way for the dominant-frequency components of vibration records to be narrowed down to dominant elements. Changes in the resonance of the structural transfer functions can be expected to be visualized even under stationary random-vibration conditions. Figure 2 shows what effect

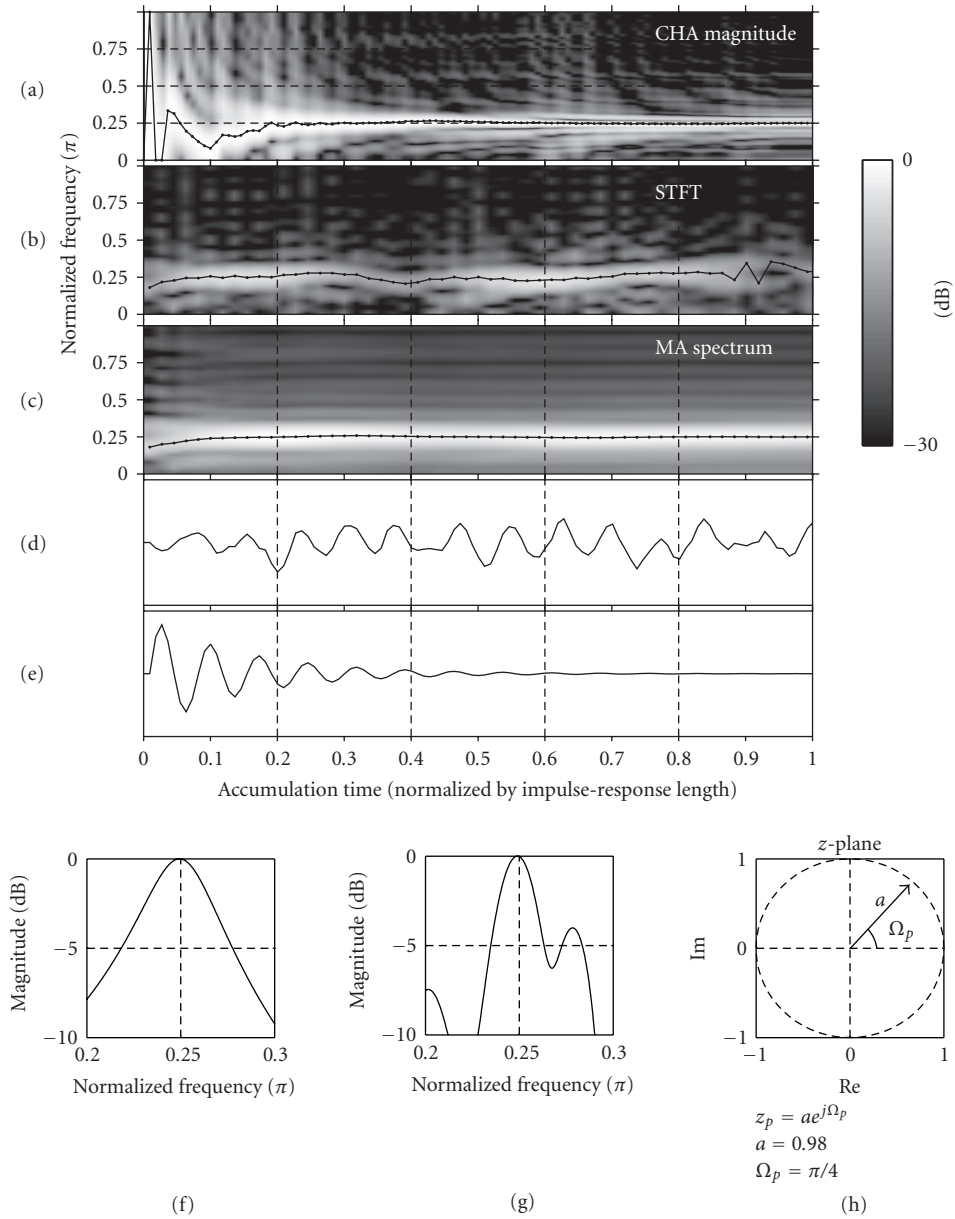

Figure 3: Examples of CHA and spectrograms for random record of single-degree-of-freedom (SDOF) system. (a) CHA magnitude and (b) spectrogram using STFT conditions are frame length, that is, 0.18 with zero padding under conditions where total Fourier-transform length is 91 and frame hop size is 1/10 frame length. Time intervals are normalized by impulse response record length (1000 points). (c) Moving averaged spectrogram using averaging STFT, (b) frame-by-frame, (d) random record to be analyzed, and (e) impulse response record of vibration system where length is defined by reverberation time. (f) Magnitude response and normalized frequency, (g) close up of CHA magnitude in (a) at final observation instant accumulation time of 1, and (h) pole plot of transfer function for impulse response in (e).

CHA has against regular DFT using real and causal sequences including complex conjugate poles. In this example, pole a in (5) has been expanded to a complex number for a more general demonstration. The locations of the complex-conjugate poles are shown in panel (d). The impulse response is illustrated in panel (a), the magnitude record for CSA is in panel (c), and that for CHA is in (b). The maximum magnitude is normalized to unity at every instant in both panels (b) and (c). We can see the spectral-accumulation process is emphasized by CHA where the resonant peak is increasing.

3. CHA EXAMPLE OF RANDOM VIBRATION RECORD IN SINGLE-DEGREE-OF-FREEDOM (SDOF) SYSTEM

Assume that we have a random vibration record observed in a single-degree-of-freedom (SDOF) system. These types of structural-vibration samples are normally easy to obtain in

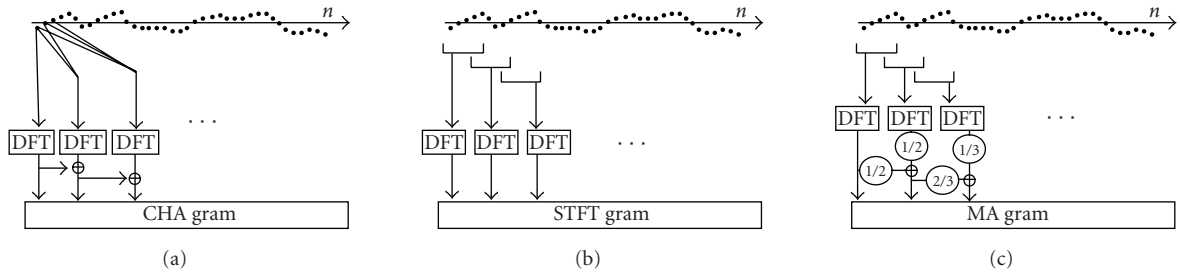

Figure 4: Algorithms for (a) CHA, (b) STFT, and (c) MA. DFT means an N-point DFT with zero padding.

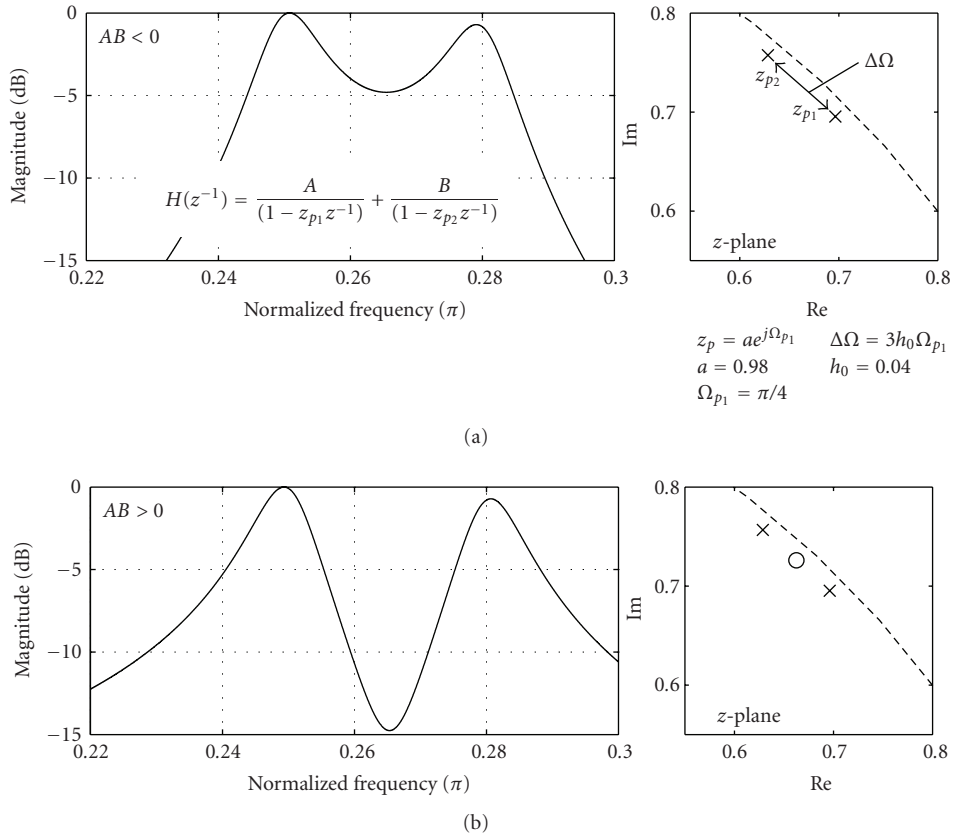

Figure 5: Pole/zero plots for two-degrees-of-freedom systems (2-DOF systems) and magnitude responses.

SIPs due to the natural force of winds, ground movement, or both [4] without specifically having to prepare source signals, which is impractical for large structures.

Figure 3 shows examples of CHA random-vibration records, including an impulse response. In the examples, we have defined the damping factor, h, as

$$h \equiv \frac{-\ln a}{\Omega_p} \cong 0.078. \tag{8}$$

The axis representing time in Figure 2 is normalized by the length of the impulse response record, which is given by the reverberation time, T_R, which is estimated as

$$T_R \equiv NT_s \cong \frac{6.9T_s}{-\ln a}. \tag{9}$$

Here, we define N as the length of an impulse response record, and T_s denotes the sampling period of discrete sequences.

In Figure 3, the CHA, STFT, and MA spectra with the peaks plots were measured on a sample-by-sample or frame-by-frame basis and the maximum magnitude records were normalized to unity in every instance of observation. We can see that CHA in panel (a) visualizes the resonant properties of the SDOF system better than the conventional spectrogram using STFT in panel (b). The spectrograms using STFT conditions are the frame length, that is, 0.18 with zero padding under conditions where the total Fourier-transform length is 91 and the frame hop size is 1/10 the frame length (the time intervals are normalized by the impulse response record length (1000 points)). The

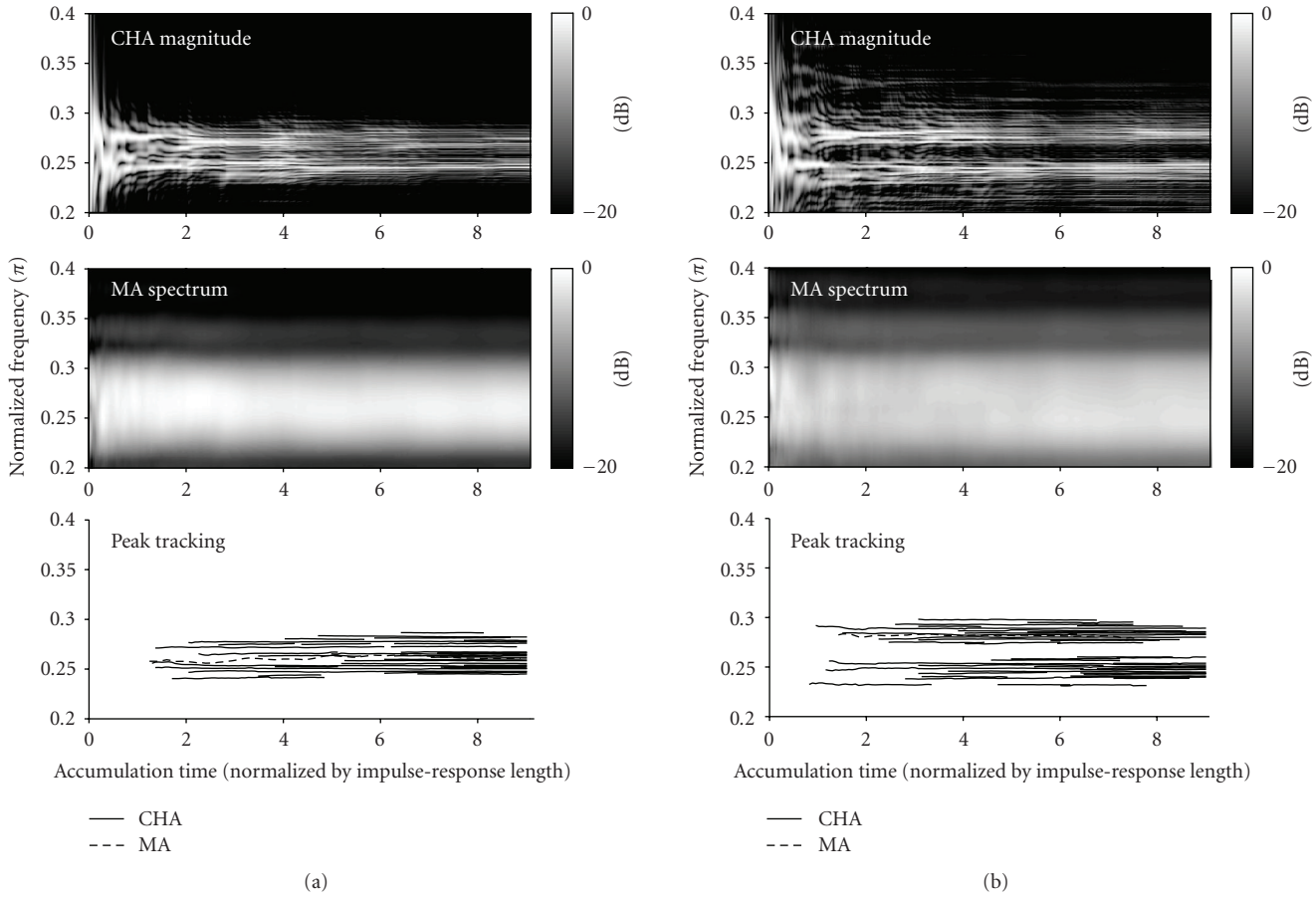

Figure 6: CHA and MA displays and tracking of prominent peaks under 2-DOF-system conditions. Panel (a): 2-DOF system without zeros, panel (b): 2-DOF system with zero.

MA spectrum in panel (c) also seems to enable stable analysis of resonant properties. The MA spectrogram uses averaging STFT frame-by-frame according to the frame progression. Panel (g) shows the CHA peak corresponding to the impulse response spectrum peak in panel (f). This means that CHA can promptly and effectively be used to determine the presumed modal frequency of the transfer function included in the noise signal. The accumulation time required to obtain a stable CHA-magnitude record seems to be around one-half the length of the impulse-response record. The spectral components of CHA obtained in every instance are interpolated by DFT with zero padding after the vibration record. Accumulating the interpolated spectra provides an accurate estimate of the modal frequency and does not suffer from the artifacts of the time-windowing function; consequently, the modal properties are emphasized by virtually increasing the degree of the pole.

4. CHA MONITORING OF MODAL OVERLAP CONDITIONS IN TWO-DEGREES-OF-FREEDOM (2-DOF) SYSTEM

The damping condition is a significant indicator of structural damage. This section explains how CHA visualizes the effect of damping on the spectral distribution. Structural-vibrating systems at low frequencies generally have low modal overlap. However, if there is a pair of adjacent poles, the damping conditions change the modal overlap, which is defined as [9, 10]

$$M \equiv \frac{B}{\overline{\Delta\omega}}, \quad B \cong \pi\delta = \pi h\omega_p, \tag{10}$$

where B is the modal bandwidth, $\overline{\Delta\omega}$ is the average modal spacing, and ω_p is the modal angular frequency of interest. Figure 5 shows examples of the pole/zero plots for a 2-DOF system under low modal-overlap conditions. Panel (b) is a plot with a single zero, and panel (a) is that without zeros between the poles. A pair of same sign residues yields a zero between the poles, and a pair of poles with different sign residues has no zeros [11–13]. Here, we set $\overline{\Delta\omega}$ as the distance between the two pole angular frequencies in Figure 5. ωp is given by Ω_{p_1}. We varied the damping conditions to control the modal overlap.

Figure 6 shows the CHA magnitudes and MA spectrums for the 2-DOF system illustrated in Figure 5. We can seen that CHA in both panels (a) and (b) visualizes the resonant properties of the 2-DOF system better than the conventional MA spectrograms. Panel (a) is a plot without zeros, and panel

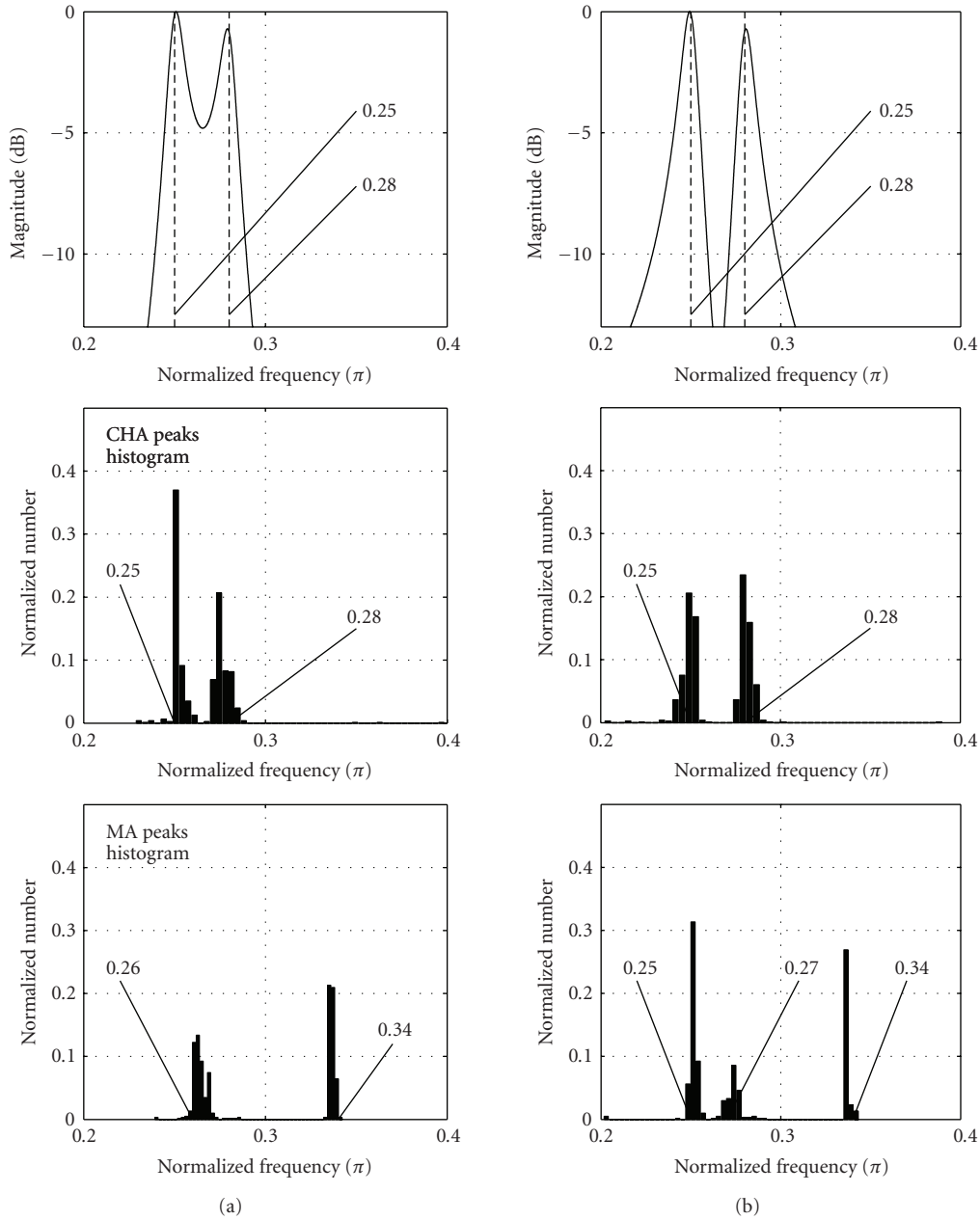

Figure 7: CHA and MA peak histogram for 2-DOF system. Panel (a): 2-DOF system without zeros, panel (b): 2-DOF system with zero.

(b) is one with a single zero. The modal overlap conditions in both panels were set to $M = 0.5$. The top and middle panels illustrate the CHA and MA records. The bottom panels in (a) or (b) show the results of spectral tracking [14] for prominent peaks of CHA or MA spectrograms. Figure 7 shows histograms of all the peaks in Figure 6. We can see that the CHA peaks correspond to the modal frequencies.

5. CHA MONITORING UNDER CONDITIONS WITH DAMPING CHANGES

This section discusses how CHA visualizes spectral changes due to damping conditions. Figure 8 shows examples of modal-overlap conditions changing from $M = 0.25$ to $M = 1$ during CHA monitoring with or without a zero between the poles. Panel (a) shows the case without zeros, and panel (b) includes a zero between the poles. The bottom panels illustrate the peak-tracking results of the CHA spectrogram. We can see that the variance in the peak-tracking lines of the CHA peaks increases according to the change in damping in both panels.

6. SUMMARY

We assessed CHA and confirmed through numerical simulation experiments that it effectively enabled system damping

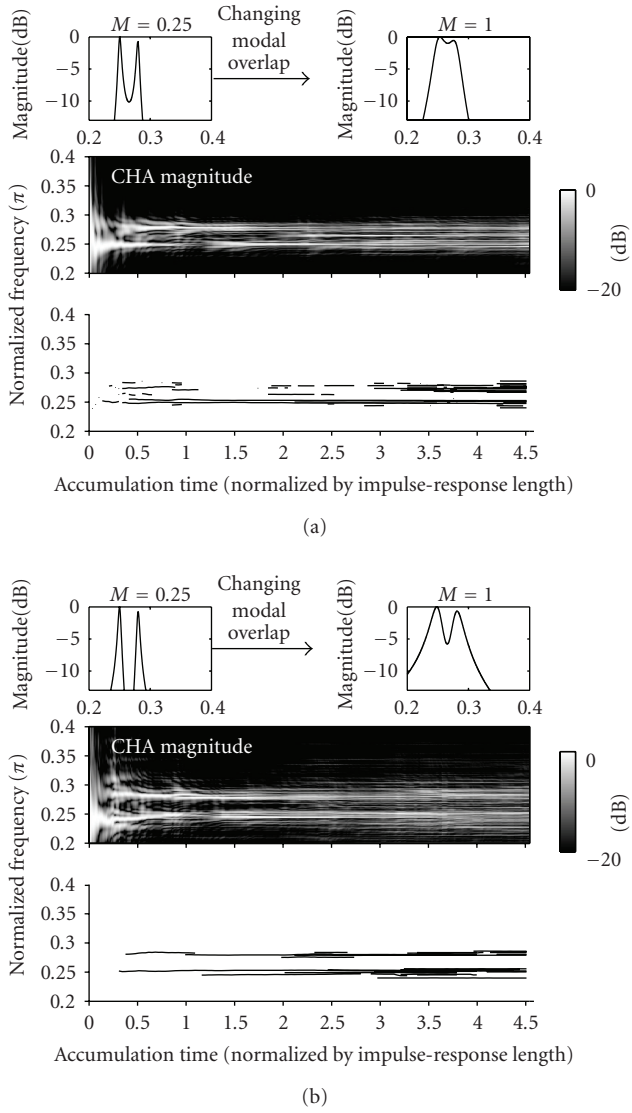

Figure 8: Modal overlap changing during CHA for 2-DOF system. Panel (a): 2-DOF system without zeros and panel (b): 2-DOF system with zero.

and modal-overlap conditions to be visualized without having to use transient-response records. We developed a potential new area in cumulative analysis by introducing a spectral-accumulation function into the conventional method proposed by Berman and Fincham. Spectral properties of the transfer function can be emphasized and visualized by using CHA-magnitude records even for short intervals of stationary random-vibration records. For simulated 2-DOF system vibration records differences and changes in the modal-overlap conditions were observable in the contour plots of the CHA magnitude as a function of time and frequency. Our computer simulation confirmed that CHA can effectively be used to estimate the damped natural frequency under SDOF conditions. The results indicate that CHA could be an efficient method of monitoring and diagnosing structures without signal-source requirements under stationary and nonstationary vibration conditions. However, substantial field tests are required to develop a more practical monitoring system.

REFERENCES

[1] Y. Takahashi, M. Tohyama, and Y. Yamasaki, "Cumulative spectral analysis for transient decaying signals in a transmission system including a feedback loop," *Journal of the Audio Engineering Society*, vol. 54, no. 7-8, pp. 620–629, 2006.

[2] P. J. Halliday and K. Grosh, "Maximum likelihood estimation of structural wave components from noisy data," *The Journal of the Acoustical Society of America*, vol. 111, no. 4, pp. 1709–1717, 2002.

[3] J. G. McDaniel and W. S. Shepard Jr., "Estimation of structural wave numbers from spatially sparse response measurements," *The Journal of the Acoustical Society of America*, vol. 108, no. 4, pp. 1674–1682, 2000.

[4] Y. Hirata, "A method for monitoring invisible changes in a structure using its non-stationary vibration," *Journal of Sound and Vibration*, vol. 270, no. 4-5, pp. 1041–1044, 2004.

[5] Y. Hirata, "Non-harmonic Fourier analysis available for detecting very low-frequency components," *Journal of Sound and Vibration*, vol. 287, no. 3, pp. 611–613, 2005.

[6] M. Kazama, K. Yoshida, and M. Tohyama, "Signal representation including waveform envelope by clustered line-spectrum modeling," *Journal of the Audio Engineering Society*, vol. 51, no. 3, pp. 123–137, 2003.

[7] J. M. Berman and L. R. Fincham, "The application of digital techniques to the measurement of loudspeakers," *Journal of the Audio Engineering Society*, vol. 25, no. 6, pp. 370–384, 1977.

[8] Y. Takahashi, M. Tohyama, M. Matsumoto, and H. Yanagawa, "An auditory events modeling language (AEML) for interactive sound field network," in *Proceedings of the 18th International Congress on Acoustics (ICA '04), Tu5.D.5*, pp. 1449–1452, Kyoto, Japan, April 2004.

[9] M. Tohyama and A. Suzuki, "Active power minimization of a sound source in a closed space," *Journal of Sound and Vibration*, vol. 119, no. 3, pp. 562–564, 1987.

[10] R. H. Lyon, "Statistical analysis of power injection and response in structures and rooms," *The Journal of the Acoustical Society of America*, vol. 45, no. 3, pp. 545–565, 1969.

[11] R. H. Lyon, "Progressive phase trends in multi-degree-of-freedom systems," *The Journal of the Acoustical Society of America*, vol. 73, no. 4, pp. 1223–1228, 1983.

[12] R. H. Lyon, "Range and frequency dependence of transfer function phase," *The Journal of the Acoustical Society of America*, vol. 76, no. 5, pp. 1433–1437, 1984.

[13] M. Tohyama and R. H. Lyon, "Zeros of a transfer function in a multi-degree-of-freedom vibrating system," *The Journal of the Acoustical Society of America*, vol. 86, no. 5, pp. 1854–1863, 1989.

[14] T. Taniguchi, M. Tohyama, and K. Shirai, "Spectral frequency tracking for classifying audio signals," in *Proceedings of the 6th IEEE International Symposium on Signal Processing and Information Technology (ISSPIT '06)*, pp. 300–303, Vancouver, Canada, August 2006.